# TRANSPORT PROPERTIES OF LATERAL SURFACE SUPERLATTICES

T. Yamada and D. K. Ferry
*Center for Solid State Electronics Research*
*Arizona State University, Tempe, AZ 85287-6206*

## Abstract

The transport properties of lateral surface superlattices, a two-dimensional (2D) electron system in a 2D periodic potential, are studied with a molecular-dynamics Monte-Carlo technique. Excellent numerical energy conservation is achieved by adopting a predictor-corrector algorithm to integrate the equations of motion. With increasing 2D potential amplitude, electrons show a transition, from a mobile phase to an immobile phase where the radial distribution function has some characteristic peaks, indicating the beginning of the long-range ordering of the electrons in the potential minima. The velocity autocorrelation function shows a 2D plasma oscillation in the mobile phase, while in the immobile phase the classical oscillation at the bottom of the potential well is observed. Raising the temperature improves the transport since electrons are released from the constraint of the 2D potential and Coulomb potential.

## Introduction

Due to the rapid progress in semiconductor technology, a two-dimensional (2D) electron gas in a 2D periodic potential with the period $a \sim 0.1$ μm can now be achieved in lateral surface superlattices (LSSLs) forming FET structures with meshed-gate electrodes [1,2]. A classical electron picture often gives a successful explanation of the experimental results at temperatures above liquid helium [3]. However, most such studies have focused on a situation where the number of electrons in a unit cell is so large that the Coulomb interaction between electrons is well screened, and as a result, a non-interacting, independent electron picture prevails. If we reduce the number of electrons in a unit cell, the screening becomes irrelevant and all the electrons are more or less bound to one another through the Coulomb interaction. The transport properties are profoundly influenced by the Coulomb interaction. We study the effect of the Coulomb interaction on transport properties in LSSL structures using a molecular-dynamics Monte Carlo technique [4].

## Simulation method

The electrons are considered as classical particles moving in the 2D potential created in a GaAs LSSL structure by $V(x,y) = V_0[\cos(2\pi x/a) + \cos(2\pi y/a) + 2]/4$ with $a = 0.16$ μm, following the experiment [2]. The potential amplitude $V_0$ is varied from 0 to 40 meV. The temperature is assumed to be 4.2 K and realistic impurity and phonon scattering is included in the ensemble Monte Carlo method in the usual way. The Coulomb interaction among electrons is treated in real space. At each time step, the Coulomb force is calculated for all electrons and this is used to update the position and momentum of each electron during the subsequent time step using the minimum image approximation [5]. Typically 32 electrons in $3 \times 3$ unit cells (electron areal density $1.4 \times 10^{14}$ m$^{-2}$) are simulated and the periodic boundary condition is imposed for this square with the edge length $L = 3a$.

In molecular dynamics, we update the position $x$ and momentum $p$ based on the predictor-corrector method with the accuracy of $(\Delta t)^2$, by

$$x(i+1) = x(i) + p(i)\Delta t + f[x(i)](\Delta t)^2/2 , \qquad (1)$$

$$p(i+1) = p(i) + \{f[x(i)] + f[x(i+1)]\}\Delta t/2 \,. \qquad (2)$$

where $x(i)$ and $p(i)$ indicate the functional values of $x(t)$ and $p(t)$ at the $i$th time step with step period $\Delta t$, and $f$ is the force depending on the electron coordinate $x$ (in the units of $m$ = 1). Equations (1) and (2) lead to five-digit accuracy in energy conservation throughout the simulation. Finding an initial condition is not trivial because of the Coulomb interaction included. We have performed a preliminary simulation to find an appropriate initial condition using a molecular dynamics Monte Carlo code but with a slight modification. It consists of adding a command to scale the momentum by $(\langle E_{kin}\rangle/k_BT)^{1/2}$ at every ~ $10^2$ time step so that the average electron energy is set to the temperature without changing the direction of electron momentum. From an ensemble of real simulations with initial conditions found by the above method, the raw data consist of each electron position and momentum at each time step. Using these values, we can evaluate the velocity autocorrelation function $\langle v_x(i)v_x(0)\rangle$, the mean-square displacement $\langle \Delta x^2(i)\rangle$, and the radial distribution function $g(r)$. We have created an Einstein plot of the mean square displacement and evaluated the diffusion constant $D$ from its temporal gradient, which can apply to interacting particles, rather than using the Green-Kubo formula.

## Results and discussion

The case of $V_0 = 0$ is studied at first, with sufficient impurity scattering assumed so that the impurity limited mobility is $\mu = 1.3 \times 10$ m$^2$/Vs and the diffusion constant is $D = 4.6 \times 10^{-3}$ m$^2$/s. Two results, the solid line with 32 electrons in 3 × 3 unit cells and the dotted line with 14 electrons in 2 × 2 unit cells are shown in Fig.1(a). There show no essential difference and the original square of 32 electrons in 3 × 3 unit cells seems reasonable. The velocity autocorrelation function is an oscillatory function with a strong decay. By Fourier transform with either a rectangular window or Blackman window, an estimation gives the period as 3.5 ± 0.2 ps. The oscillation is attributed to the 2D plasma oscillation with the dispersion $\omega_{2D} = (e^2 n_{2D} q/2\varepsilon m)^{1/2}$ at $q \sim (\pi n_{2D})^{1/2}$, where the dispersion becomes almost flat [6]. This is consistent with the fact that the 3D plasma oscillation has a flat dispersion part around $q \sim 0$ and a single electron couples with this mode. The time period for the present situation is estimated to be ~ 3.5 ps, consistent with the observed data.

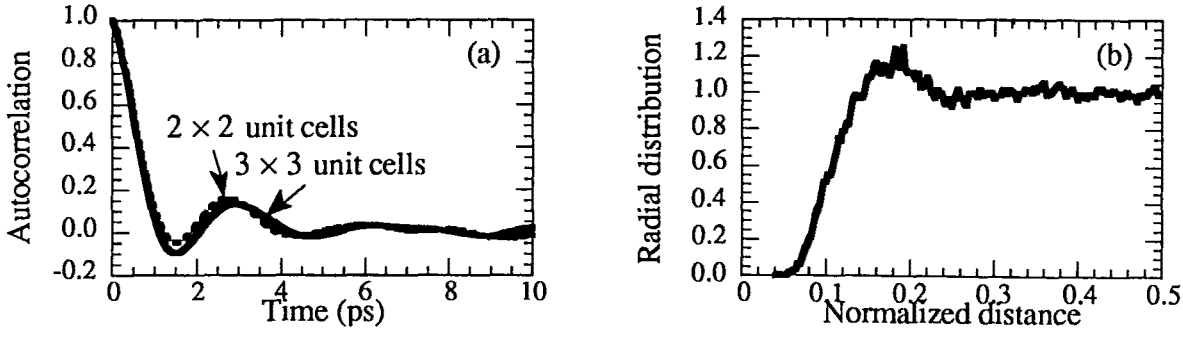


FIG.1. Simulation result with $V_0$ = 0 meV. (a) Normalized velocity autocorrelation and (b) radial distribution function.

The mean square displacement for these two cases shows a linear dependence on time with no essential difference observable. The diffusion constant $D$ is 6.7 × $10^{-4}$ m$^2$/s, which is smaller than the value with impurity scattering alone. This is a natural conclusion for the present case with the plasma coupling constant $\Gamma = e^2/(4\pi\varepsilon\lambda k_BT) = 6.43$ where $\lambda = (\pi n)^{-1/2}$ if we remember that the phase transition from the mobile phase to immobile Wigner crystal phase occurs as $\Gamma$ increases, at around $\Gamma$ ~ $10^2$ [7]. Figure 1(b) shows the radial distribution function where the distance is normalized to $L$.

The radial distribution has essentially zero value for short distances but rises rapidly and peaks around $1/\sqrt{32} = 0.177$, which is the average distance assuming a perfectly uniform 2D electron gas. As the distance increases, the radial distribution function approaches unity without showing an oscillation. This is further evidence that the electrons are in a uniform, mobile phase.

Figure 2(a) shows the velocity autocorrelation for three potential values, 2.5 meV, 5 meV, and 10 meV. The velocity autocorrelation function begins to show an oscillation with shorter time periods than that in the presence of the Coulomb interaction alone seen above. This oscillation can be attributed to a classical oscillation in the potential. For $V_0$ = 10 meV, a clear oscillation is observed, which indicates electrons are beginning to be confined in the potential minima and the major force dominating electron motion changes from Coulomb force to 2D potential force. The Fourier transform shows a peak corresponding to the time period 2.2 ps. The classical oscillation period in the potential well can be estimated numerically by integrating $1/v$ with respect to space. It gives $T_{class}$ = 2.43 ps, recovering the observed value. We have a linear time dependence of the mean square displacement and the diffusion constant is $D = 6.1 \times 10^{-4}$ m$^2$/s for $V_0$ = 2.5 meV, $D = 2.5 \times 10^{-4}$ m$^2$/s for $V_0$ = 5 meV, and $D = 6 \times 10^{-5}$ m$^2$/s for $V_0$ = 10 meV. Figure 2(b) shows radial distribution functions. For clarity, the functions for $V_0$ = 5 and 10 meV are offset by 1 and 2 units. The first peak of the radial distribution function shifts to a smaller distance with increasing potential, due to the increasing confining effect in a unit cell. The electrons do not prefer to stay around the normalized distance of 1/6, where the potential barrier appears, with increasing potential. The second peak for the normalized distance of 1/3 becomes higher and corresponds to the 2D potential period, further indicating confinement.

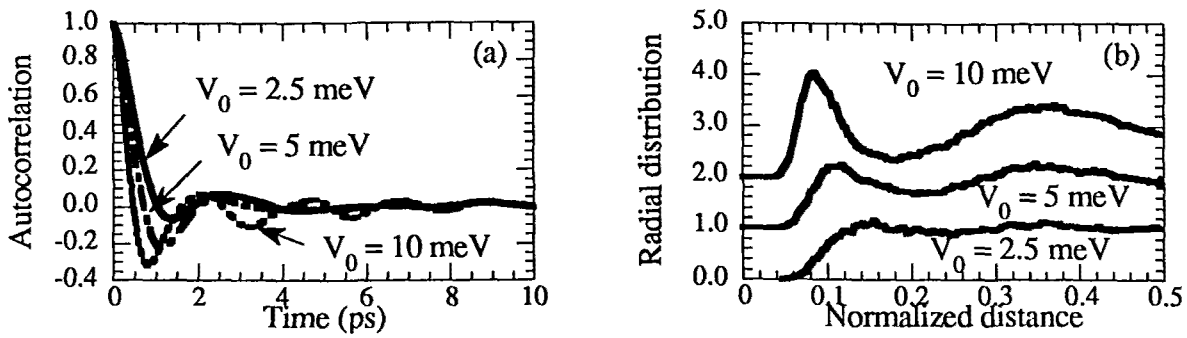


FIG.2. Simulation results with $V_0$ = 2.5, 5, and 10 meV. (a) Normalized velocity autocorrelation function and (b) radial distribution function.

When $V_0$ = 40 meV, electrons have already made a phase transition to the localized state. They oscillate at the bottom of the potential minima and none can overcome the barrier. The velocity autocorrelation in Fig.3(a) has a clear oscillation period. The Fourier transform has a peak corresponding to a time period 1.1 ps. We estimate the classical oscillation period at the potential minima numerically and find $T_{class}$ = 1.10 ps. The mean square displacement is a bounded function of time and therefore the diffusion constant is zero. The sum of average kinetic and 2D potential energy is around 3.3 meV, which is much smaller than the saddle point energy of 20 meV. Practically, it is impossible for electrons to overcome the barrier at this low temperature of 4.2 K. Coulomb energy becomes the highest contribution because of the strong spatial confinement of electrons in the potential minima. This is why the radial distribution function in Fig.3(b) shows a high first peak corresponding to the mean distance of electrons in a unit cell, followed by an essentially zero region due to high potential barrier, and the second peak corresponding to the 2D potential period at the normalized distance of 1/3. The third peak at the normalized distance at $\sqrt{2}/3$ is due to the 2D square-ordered structure in the diagonal direction.

The effect of raising the temperature is obvious. As long as phonon scattering remains small, a higher temperature causes improvement in transport since electrons have more energy to overcome the 2D potential barrier or Coulomb potential barrier. In order to show this, we have simulated several temperature points between 4.2 and 22 K for $V_0$ = 2.5 meV. The velocity autocorrelation function begins to show a simple monotonic decay, rather than an oscillation with temperature. With increasing kinetic energy, the coherent collective oscillation is disturbed and the oscillation in the velocity autocorrelation function becomes weaker. The radial distribution function approaches that of non-interacting particles with temperature. The diffusion constant is also getting larger with temperature. By creating a plot of ln($D$) versus inverse temperature $1/T$, we can estimate an activation energy. By calculating the gradient, the activation energy is ~ 1.0 meV, on the order of $V_0$.

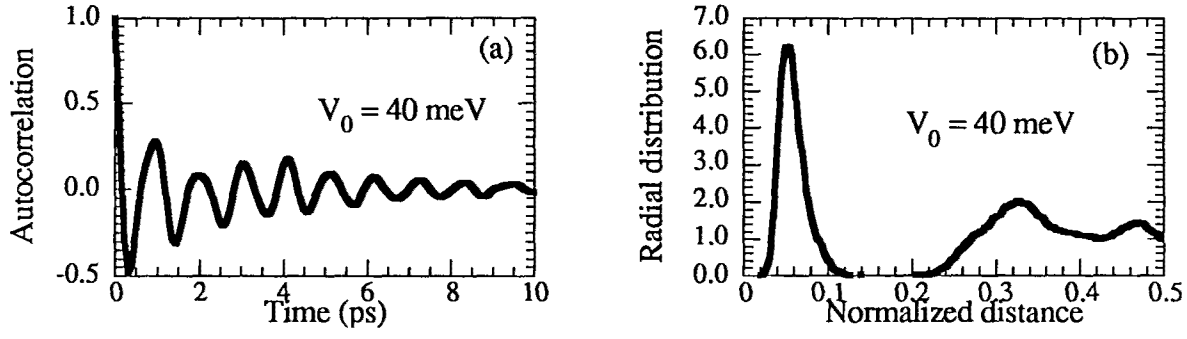


FIG.3. Simulation results with $V_0$ = 40 meV. (a) Normalized velocity autocorrelation function and (b) radial distribution function.

## Acknowledgment

Authors are grateful to A. M. Kriman for useful discussions. This work is supported by the Office of Naval Research.

## References

1. See for example,*Granular Nanoelectronics*, edited by D. K. Ferry, J. R. Barker, and C. Jacoboni, Plenum, New York (1990).
2. E. Paris, J. Ma, A. M. Kriman, D. K. Ferry, and E. Barbier, *J. Phys. Condens. Matter* **3**, 6605 (1991); J. Ma, R. A. Puechner, W.-P. Liu, A. M. Kriman, G. N. Maracas, and D. K. Ferry, *Surf. Sci.* **229**, 341 (1990).
3. C. W. J. Beenakker, *Phys. Rev. Lett.* **62**, 2020 (1989); C. W. J. Beenakker and H. van Houten, *Phys. Rev. Lett.* **63**, 1857 (1989); D. Weiss, M. L. Roukes, A. Menschig, P. Grambow, K. v. Klitzing, and G. Weimann, *Phys. Rev. Lett.* **66**, 2790 (1991).
4. P. Lugli and D. K. Ferry, *Phys. Rev. Lett.* **56**, 1295 (1986); D. K. Ferry, *Semiconductors*, Macmillan, New York (1991).
5. M. P. Allen and D. J. Tildesley, *Computer Simulation of Liquids*, Clarendon Press, Oxford (1987).
6. J. P. Hansen, D. Levesque, and J. J. Weis, *Phys. Rev. Lett.* **43**, 979 (1979); R. K. Kalia, P. Vashishta, S. W. de Leeuw, and A. Rahman, *J. Phys. C***14**, L911 (1981).
7. R. C. Gann, S. Chakravarty, and G. V. Chester, *Phys. Rev. B***20**, 326 (1979).